SPECIAL PROJECT PROGRESS REPORT

Progress Reports should be 2 to 10 pages in length, depending on importance of the project. All the following mandatory information needs to be provided.

Reporting year
2016

Project Title:
Support Tool for HALO Missions

Computer Project Account:
SPDEHALO

Principal Investigator(s):
Dr. Andreas Dörnbrack
Dr. Marc Rautenhaus
Dr. Andreas Schäfler
Sonja Gisinger
Martina Bramberger
Dr. Benedikt Ehard

Affiliation:
DLR Oberpfaffenhofen,
Institut für Physik der Atmosphäre

Name of ECMWF scientist(s) collaborating to the project
(if applicable)
Sylvie Malardel
Nils Wedi

Start date of the project:
2015

Expected end date:
2018

Computer resources allocated/used for the current year and the previous one
(if applicable)
Please answer for all project resources

		Previous year		Current year	
		Allocated	Used	Allocated	Used
High Performance Computing Facility	(units)	100000	0	100000	50000
Data storage capacity	(Gbytes)	80	80	80	80

Summary of project objectives

(10 lines max)

High-quality meteorological forecast and analysis products are essential for the successful planning and evaluation of airborne measurements. The novel and outstanding research possibilities offered by the German High Altitude and Long Range (HALO) research aircraft dedicated for atmospheric and geophysical research prompt the development of an innovative instrument in support of HALO missions. This special project is dedicated to access ECMWF's meteorological forecast and analysis products for developing and deploying such a mission support tool.

Summary of problems encountered

none

Summary of results of the current year

(1) Aircraft missions 2016

In the year 2016, two large aircraft missions with different science foci were conducted and supported by the special project scientists. POLSTRACC/SALSA/GW-LCYCLE 2[1] and NAWDEX[2] were international field campaigns combining the two research aircraft HALO and the DLR Falcon together with ground-based and airborne instrumentations provided by a variety of partners. For both missions, the customized forecasts tools were used for flight planning. For example, the Mission Support System was used via the MSS-website[3] where standardized products of the IFS high-resolution prediction were displayed.

Additionally, extensive use of the interactive Mission Support System was made to design optimal flight routes over the northern Atlantic for NAWDEX. A new component was the use of the Graphical Turbulence Guidance System (GTG) developed by Bob Sharman, NCAR (Sharman, R. D., C. Tebaldi, G. Wiener, and J. Wolff, 2006: An integrated approach to mid- and upper-level turbulence forecasting. *Wea. Forecasting*, **21**, 268–287, doi:10.1175/WAF924.1.). The GTG was installed on ECMWF's Linux cluster Ecgate and it was run in operational mode during both field campaigns. The visualisation of forecast products for clear-air turbulence (CAT) and mountain wave turbulence helped to identify scientifically interesting regions for studying instability processes in the free atmosphere and to analyse unexpected encounters with CAT.

Figure 1 shows an example of predicted mountain wave and clear-air turbulence along the flight track of HALO during the transfer flight from Oberpfaffenhofen to Kiruna (via Malta) on 12 January 2016. Over the Apennine Mountains, HALO encountered light turbulence due to breaking mountain waves. Additionally, the large amplitude mountain waves led to local cooling of the stratospheric air and HALO entered a hazardous flight situation. Currently, Martina Bramberger investigates this case in more detail.

[1] https://www.polstracc.kit.edu/polstracc/index.php/POLSTRACC
[2] http://www.pa.op.dlr.de/nawdex
[3] http://www.pa.op.dlr.de/missionsupport/classic/forecasts/

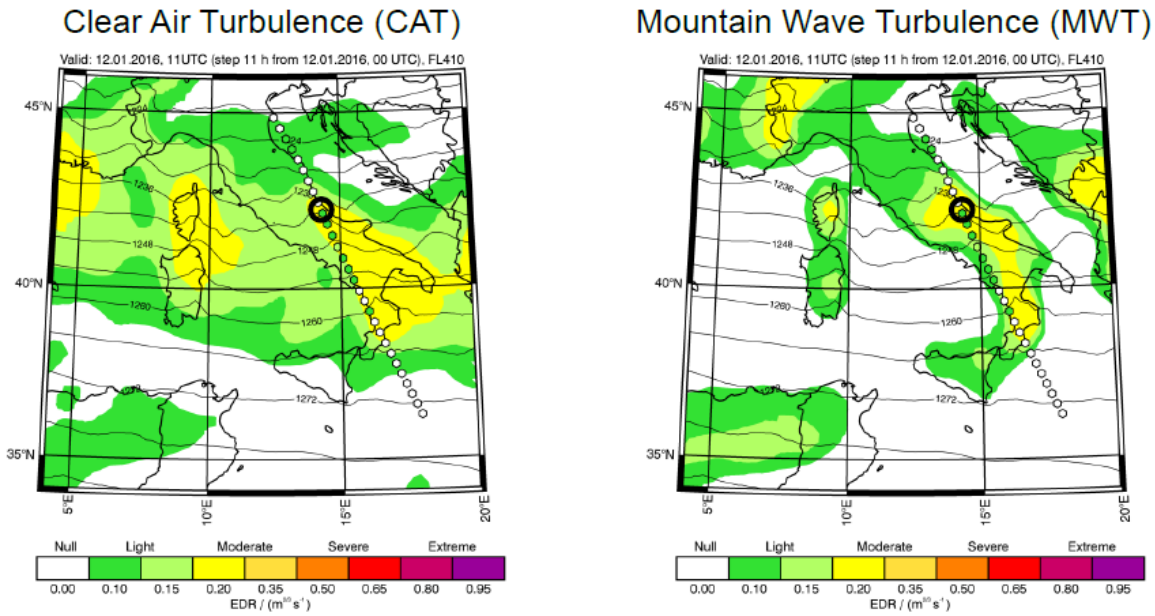

Figure 1: Regions of predicted clear-air turbulence and mountain wave turbulence at FL 410 over Italy on 12 January 2016. Predictions by the GTG forced my ECMWF IFS high resolution forecasts. The dotted lines mark the aircraft flight track, the enhanced bold circle the location of observed turbulence encounter.

(2) Publications

ECMWF IFS and ERA-Interim data were used in a couple of publications (numbers 1-6, 8-11, 14-17, and 19 in the reference list provided below) devoted to the deep vertical propagation of mountain waves over New Zealand during DEEPWAVE, GW-LCYCLE 1 and POLSTRACC/SALSA/GW-LCYCLE 2 missions as well as other applications from field observations. Most of the paper are accepted, some undergo minor revisions.

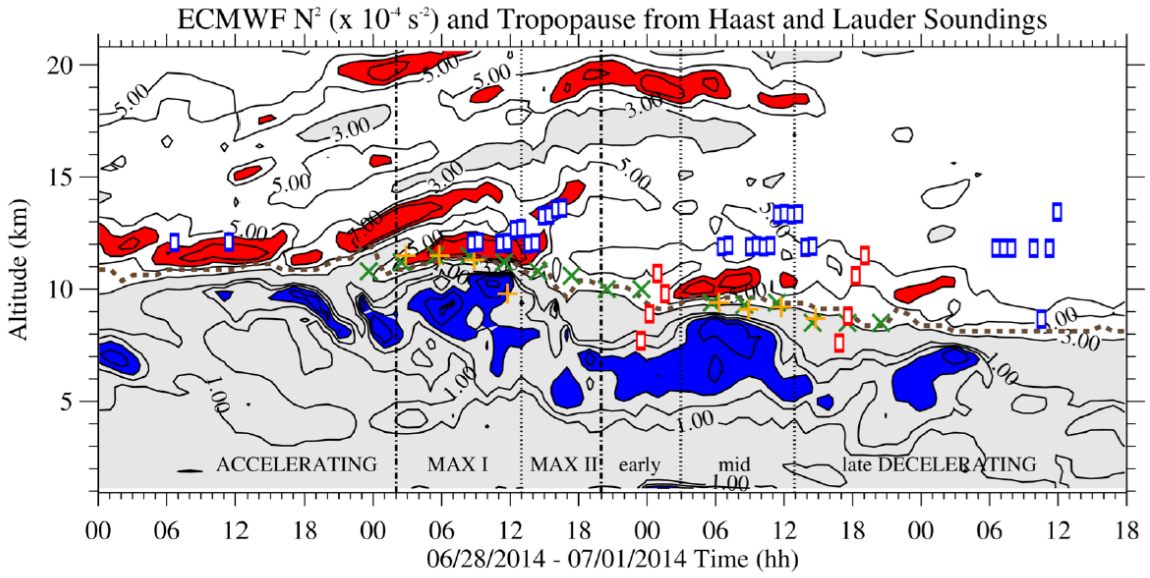

Figure 2:Composite depicting the temporal evolution of the conditions in the vicinity of the tropopause during the different phases of the observed transient mountain wave event. ECMWF IFS Brunt-Vaisala frequency (N^2) with coloured contours of $\geq 6 \cdot 10^{-4}$ s^{-2} in red and $\leq 0.5 \cdot 10^{-4}$ s^{-2} in blue. Grey shaded are areas of $N^2 \leq 3 \cdot 10^{-4}$ s^{-2}. The brown dashed line, the orange normal and green diagonal crosses give the thermal tropopause calculated from ECMWF, as well as from Haast and Lauder soundings, respectively. Blue and red rectangles show altitudes of all GV and Falcon mountain legs. Dotted-dashed vertical lines are the separation into accelerating, maximum and decelerating forcing phases. Dotted vertical lines further show the division into maximum forcing phase I and II, and early, mid and late decelerating forcing phases.

One highlight is the study of Portele et al. (Portele, T. C., A. Dörnbrack, B. & N. Kaifler, J. S. Wagner, P.-D. Pautet, and Markus Rapp, 2017: Mountain Wave Propagation under Transient Tropospheric Forcing: A DEEPWAVE Case Study. Mon. Wea. Rev., under revision) where a mountain wave case under transient tropospheric forcing is investigated in great detail. To investigate the impact of the transient forcing on the deep vertical gravity wave propagation, results of different observational sensors and numerical modelling were combined (Figure 2). A slowly eastward-migrating through, including crossing frontal systems over the South Island of New Zealand controlled the upstream low-level wind following approximately a cos2 shape. Vertical energy fluxes (EF_z) and amplitudes of vertical displacements of air parcels in the upper troposphere and lower stratosphere (UTLS) went up to 4000 kW m^{-1} and 1500 m, respectively. Their temporal evolution was phase-shifted to the cos^2-shape by about 8 hours and influenced by the temporally varying propagation conditions in the UTLS. It was further shown that this time evolution of EF_z can be described by a sequence of EF_z-values of individual quasi-stationary states. Shorter waves ($\lambda_x \approx 20 \ldots 30$ km) were continuously forced during the event and their vertical propagation varied in response to the conditions in the UTLS. Longer waves were only excited during maximum flow over the envelope of the Southern Alps and

propagated deeply into the mesosphere. Their long propagation time of about 10 to 24 h caused a retarded enhancement of mesospheric gravity wave activity about 24 hours after the maximum tropospheric forcing.

Special attention should be given to the study by B. Ehard (Ehard, B., S. Malardel, A. Dörnbrack, B. Kaifler, N. Kaifler, and N. Wedi, 2017: Comparing ECMWF high resolution analyses to lidar temperature measurements in the middle atmosphere. submitted to Q. J. R. Met. Soc.). In this paper, middle atmospheric lidar temperature observations conducted during the GW-LCYCLE 2 campaign in December 2015 above Finland are compared to two sets of simulations by IFS. One of the simulations is the operational cycle 41r1 with a horizontal resolution of 16 km and the other is the e-Suite 69 (later cycle 41r2) with a 9 km horizontal resolution. A remarkable agreement between both ECMWF IFS simulations and the lidar temperature observations is found below 45 km altitude (Figure 3). Above 45 km altitude, within the sponge layer of the ECMWF IFS, both simulations depict lower temperatures than the observations, with the high-resolved ECMWF IFS version showing the largest cold bias. Test runs of the ECMWF IFS are analysed and compared to the lidar observations to investigate the effect of the high-resolution horizontal grid.

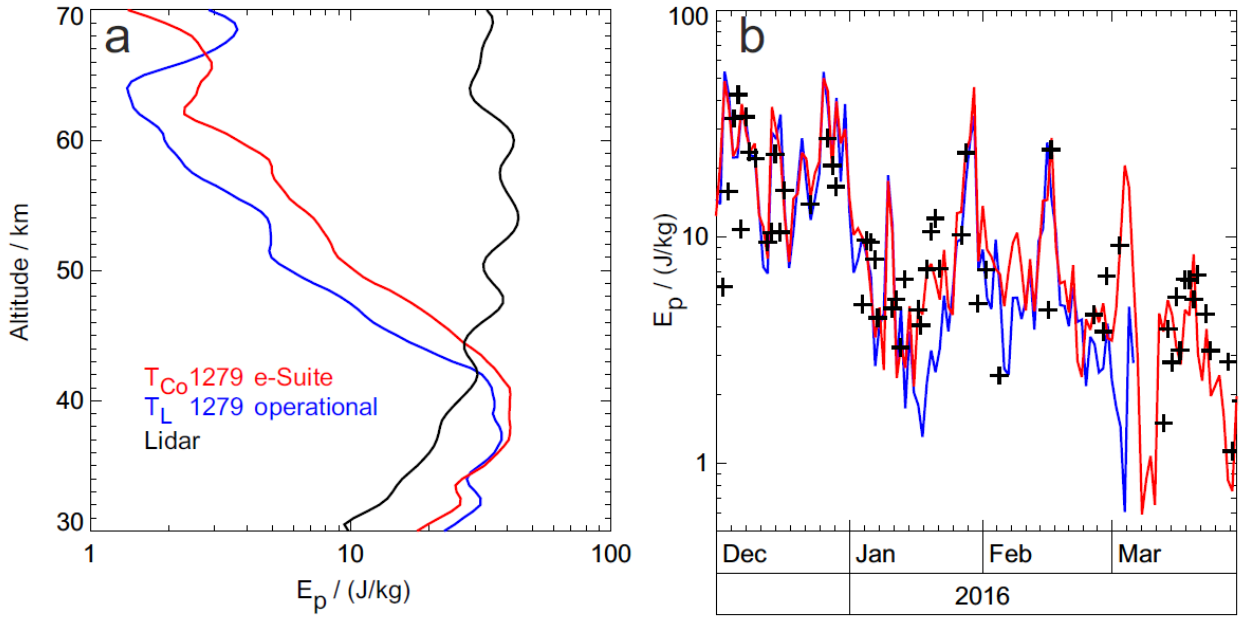

Figure 3. Left panel: Mean gravity wave potential energy density E_p above Sodankylä, Finland, during December 2015 derived from CORAL measurements (black), the operational ECMWF IFS cycle 41r1 (blue) and the e-Suite 69 (red). Only ECMWF IFS profiles with simultaneous lidar measurements were used. Right panel: Daily mean E_p between 30 and 40 km altitude over Sodankylä derived from CORAL measurements (black crosses), operational ECMWF IFS cycle 41r1 simulations (T_L1279, blue line) and e-Suite 69 simulations (T_{Co}1279, red line). Here all ECMWF IFS profiles above Sodankylä from December 2015 to March 2016 were used.

Figure 3: Figure 3 taken from Ehard et al. (2017) documenting both the astonishing agreement between the ECMWF IFS predictions in layers below 45 km altitude and the enormous differences in gravity wave potential energy above that altitude.

An interesting application of the ECMWF IFS data is the study by Ulrich Schumann (Giez et al., 2017:). It shows impressively how ECMWF IFS data can be used to “calibrate” the pressure sensors of aircraft: Accurate static-pressure measurements are a prerequisite for safe navigation and precise air-data measurements on aircraft. Pressure is also fundamental for wind and air temperature analysis in meteorology. Static-pressure measurement by aircraft is disturbed by aerodynamics and needs to be corrected using calibration. In this paper, a comparison has been made between static pressure measured by means of a

trailing cone in the atmosphere behind two different jet aircraft at flight levels up to 450 and data from numerical weather predictions. The height is derived from differential Global Navigation Satellite System measurements. The Global Navigation Satellite System height is compared to numerical-weather-prediction geopotential height. The numerical-weather-prediction data were provided by the Integrated Forecast System of the European Centre for Medium-Range Weather Forecasts. When computing the geopotential with latitude-/height-dependent gravity, the pressure/height differences are -0.01 ± 0.15 hPa and 0.6 ± 0.2 m. This pressure accuracy implies numerical-weather-prediction temperature errors < 0.1 K on average below 10 km altitude. The trailing-cone measurements provide a first quantification of the case-specific accuracy of numerical-weather-prediction pressure–geopotential relationships. The method of comparing operational pressure/Global Navigation Satellite System measurements on aircraft with numerical-weather-prediction analysis or predictions can be used to test the height-keeping performance of aircraft after or during operation

List of publications/reports from the project with complete references

Members of the Special Project are highlighted in the author's lists.

1. **Bramberger, M.**, **A. Dörnbrack**, K. Bossert, **B. Ehard**, D. C. Fritts, B. Kaifler, C. Mallaun, A. Orr, P.-D. Pautet, M. Rapp, M. J. Taylor, S. Vosper, B. Williams, and B. Witschas, 2017: Does strong tropospheric forcing cause large-amplitude mesospheric gravity waves? - A DEEPWAVE Case Study. *J. Geophys. Res*., under review.

2. **Ehard, B**., S. Malardel, **A. Dörnbrack**, B. Kaifler, N. Kaifler, and N. Wedi, 2017: Comparing ECMWF high resolution analyses to lidar temperature measurements in the middle atmosphere. submitted to *Q. J. R. Met. Soc*. 16.4.2017

3. Heller, R., C. Voigt, S. Kaufmann, **A. Dörnbrack**, J. Wagner, H. Schlager, S. Beaton, K. Young, and M. Rapp, 2017: Mountain waves modulate the water vapour distribution in the UTLS, *Atmos. Chem. Phys*., under review..

4. Krisch, I., Preusse, P., Ungermann, J., **Dörnbrack, A**., Eckermann, S. D., Ern, M., Friedl-Vallon, F., Kaufmann, M., Oelhaf, H., Rapp, M., Strube, C., and Riese, M.: First tomographic observations of gravity waves by the infrared limb imager GLORIA, *Atmos. Chem. Phys. Discuss*., https://doi.org/10.5194/acp-2017-644, in review, 2017

5. Portele, T. C., **A. Dörnbrack**, B. & N. Kaifler, J. S. Wagner, P.-D. Pautet, and Markus Rapp, 2017: Mountain Wave Propagation under Transient Tropospheric Forcing: A DEEPWAVE Case Study. *Mon. Wea. Rev*., under revision

6. **Gisinger, S**., **A. Dörnbrack**, V. Matthias, J. D. Doyle, S. D. Eckermann, **B. Ehard**, L. Hoffmann, B. Kaifler, C. G. Kruse, and M. Rapp, 2016: Atmospheric Conditions during the Deep Propagating Gravity Wave Experiment (DEEPWAVE), *Mon. Wea. Rev*., EOR: https://doi.org/10.1175/MWR-D-16-0435.1

7. Witschas, B., S. Rahm, **A. Dörnbrack**, J. Wagner, and M. Rapp, 2017: Airborne Coherent Doppler Wind Lidar measurements of vertical and horizontal winds for the investigation of orographically induced gravity waves. *J. Atmos. Oceanic Technol*., **34**, 1371–1386, https://doi.org/10.1175/JTECH-D-17-0021.1

8. Zhao, J., X. Chu, C. Chen, X. Lu, W. Fong, Z. Yu, R M. Jones, B. R. Roberts, and **A. Dörnbrack**, 2017: Lidar observations of stratospheric gravity waves from 2011 to 2015 at McMurdo (77.84° S, 166.69° E), Antarctica: Part I. Vertical wavelengths, periods, and frequency and vertical wavenumber spectra. *J. Geophys. Res. Atmos.*, **122**, 5041–5062, *doi:*10.1002/2016JD026368.

9. Jurkat, T., C. Voigt, S. Kaufmann, J.-U. Grooß, H. Ziereis, **A. Dörnbrack**, P. Hoor, H. Bozem, A. Engel, H. Bönisch, T. Keber, T. Hüneke, K. Pfeilsticker, A. Zahn, K. Walker, C.D. Boone, P.F. Bernath, and H. Schlager, 2017: Depletion of ozone and reservoir species of chlorine and nitrogen oxide in the lower Antarctic polar vortex measured from aircraft. *Geophys. Res. Lett.*, **44**, DOI: 10.1002/2017GL073270

10. Kaifler, N., Kaifler, B., **Ehard, B.**, **Gisinger, S., Dörnbrack, A.**, Rapp, M.,Kivi, R., Kozlovsky, A., Lester, M., and Liley, B., 2017: Observational indications of downward-propagating gravity waves in middle atmosphere lidar data, *Journal of Atmospheric and Solar-Terrestrial Physics*, EOR: https://doi.org/10.1016/j.jastp.2017.03.003

11. Wagner, J., **Dörnbrack, A.**, Rapp, M., **Gisinger, S.**, **Ehard, B.**, **Bramberger, M.**, Witschas, B., Chouza, F., Rahm, S., Mallaun, C., Baumgarten, G., and Hoor, P., 2017: Observed versus simulated mountain waves over Scandinavia – improvement of vertical winds, energy and momentum fluxes by enhanced model resolution?, *Atmos. Chem. Phys.*, **17**, 4031-4052, doi:10.5194/acp-17-4031-2017.

12. Voigt, C., U. Schumann, A. Minikin, A. Abdelmonem, A. Afchine, S. Borrmann, M. Boettcher, B. Buchholz, L. Bugliaro, A. Costa, J. Curtius, M. Dollner, **A. Dörnbrack**, V. Dreiling, V. Ebert, A. Ehrlich, A. Fix, L. Forster, F. Frank, D. Fütterer, A. Giez, K. Graf, J. Grooß, S. Groß, K. Heimerl, B. Heinold, T. Hüneke, E. Järvinen, T. Jurkat, S. Kaufmann, M. Kenntner, M. Klingebiel, T. Klimach, R. Kohl, M. Krämer, T. Krisna, A. Luebke, B. Mayer, S. Mertes, S. Molleker, A. Petzold, K. Pfeilsticker, M. Port, M. Rapp, P. Reutter, C. Rolf, D. Rose, D. Sauer, A. Schäfler, R. Schlage, M. Schnaiter, J. Schneider, N. Spelten, P. Spichtinger, P. Stock, A. Walser, R. Weigel, B. Weinzierl, M. Wendisch, F. Werner, H. Wernli, M. Wirth, A. Zahn, H. Ziereis, and M. Zöger, 2017: ML-CIRRUS: The Airborne Experiment on Natural Cirrus and Contrail Cirrus with the High-Altitude Long-Range Research Aircraft HALO. *Bull. Amer. Meteor. Soc.*, **98**, 271–288, doi: 10.1175/BAMS-D-15-00213.1.

13. **Dörnbrack, A.**, **S. Gisinger**, and B. Kaifler, 2017: On the Interpretation of Gravity Wave Measurements by Ground-Based Lidars. *Atmosphere*, **8**, 1–22. DOI: 10.3390/atmos8030049 ISSN 2073-443

14. **Dörnbrack, A.**, **S. Gisinger**, M. C. Pitts, L. R. Poole, and M. Maturilli, 2017: Multilevel cloud structure over Svalbard, *Mon. Wea. Rev.*, **145**, 1149–1159, doi: 10.1175/MWR-D-16-0214.1.

15. Giez, A., Mallaun, C., Zöger, M., **Dörnbrack, A.**, and Schumann, U., 2017: Static Pressure from Aircraft Trailing-Cone Measurements and Numerical Weather-Prediction Analysis. *Journal of Aircraft*. DOI: 110.2514/1.C034084 ISSN 0021-8669

16. **Ehard, B.**, B. Kaifler, **A. Dörnbrack**, P. Preusse, S. D. Eckermann, **M. Bramberger, S. Gisinger**, N. Kaifler, B. Liley, J. Wagner, and M. Rapp, 2017: Horizontal propagation of large-amplitude mountain waves in the vicinity of the polar night jet, *J. Geophys. Res.*, *Atmos.*, **122**, doi:10.1002/2016JD025621

17. Matthias, V., **A. Dörnbrack**, and G. Stober, 2016: The extraordinarily strong and cold polar vortex in the early northern winter 2015/16, *Geophys. Res. Lett.*, **43**, doi:10.1002/2016GL071676.

18. Smith, R. B., A. D. Nugent, C. G. Kruse, D. C. Fritts, J. D. Doyle, S. D. Eckermann, M. J. Taylor, **A. Dörnbrack**, M. Uddstrom , W. Cooper, P, Romashkin, J. Jensen, S. Beaton, 2016: Stratospheric Gravity Wave Fluxes and Scales during DEEPWAVE, *J. Atmos. Sci.*, **73**, 2851–2869, DOI: http://dx.doi.org/10.1175/JAS-D-15-0324.1

19. Fritts, D. C., R. B. Smith, M. J. Taylor, J. D. Doyle, S. D. Eckermann, **A. Dörnbrack**, M. Rapp, B. P. Williams, P.-D. Pautet, K. Bossert, N. R. Criddle, C. A. Reynolds, P. A. Reinecke, M. Uddstrom, M. J. Revell, R. Turner, B. Kaifler, J. S. Wagner, T. Mixa, C. G. Kruse, A. D. Nugent, C. D. Watson, **S. Gisinger**, S. M. Smith, R. S. Lieberman, B. Laughman, J. J. Moore, W. O. Brown, J. A. Haggerty, A. Rockwell, G. J. Stossmeister, S. F. Williams, G. Hernandez, D. J. Murphy, A. R. Klekociuk, I. M. Reid, and J. Ma, 2016: The Deep Propagating Gravity Wave Experiment (DEEPWAVE): An Airborne and Ground-Based Exploration of Gravity Wave Propagation and Effects from their Sources throughout the Lower and Middle Atmosphere, *Bull. Am. Meteorol. Soc.*, **97**, 425–453 doi:10.1175/BAMS-D-14-00269.1.

20. **Ehard, B.**, P. Achtert, **A. Dörnbrack**, **S. Gisinger**, J. Gumbel, M. Khaplanov, M. Rapp, and J. Wagner, 2016: Combination of lidar and model data for studying deep gravity wave propagation, Combination of Lidar and Model Data for Studying Deep Gravity Wave Propagation. *Mon. Wea. Rev.*, **144**, 77–98. doi: http://dx.doi.org/10.1175/MWR-D-14-00405.1

Summary of plans for the continuation of the project

Full concentration further goes to the publication of the results of the previous campaigns. Numerical simulations with the all-scale geophysical flow solver EULAG will be conducted to facilitate the interpretation of the observations.